# Isolated galaxies in observations and simulations

Sergey Pilipenko spilipenko@asc.rssi.ru
Andrei Doroshkevich dorr@asc.rssi.ru

Lebedev Physical Institute

## Abstract

A comparison of observed and simulated isolated galaxies allows us to check their evolution in a wide range of redshifts and to reveal and evaluate a possible impact of their environment. Using the Minimal Spanning Tree (MST) technique we select samples of isolated galaxies, pairs and groups in the SDSS DR7 and in the high resolution dark matter simulation which is a part of the Marenostrum Universe Project. The evolution of isolated simulated halos is described as a function of redshift and selection parameters. The analysis of samples of isolated objects is complemented by the study of LSS also selected with the MST and dynamical properties of environment (in simulation only). For SDSS galaxies we plot luminocity functions and $u-z$ color histograms.

We find that the separation to the nearest neighbour should be $4-5\,h^{-1}$ Mpc to produce a sample of isolated objects with substantially peculiar environment.

## Introduction

The analysis of the percolation process demonstrates that in both observed and simulated catalogs **there is one multiconnected void** and a joint complex network of the LSS elements — walls, filaments and separate objects (galaxies, DM halos or DM particles). Therefore the spatial distribution of the matter is characterized mainly by properties of these structure elements.

The most general characteristic of the LSS is the **Minimal Spanning Tree (MST)** which links all objects of the sample in joint tree. It allows to separate high and low density regions, to discriminate approximately between the separate structure elements and to determine their characteristics. The mean characteristics of simulated walls – the surface density of objects, wall separation and velocity, and the velocity dispersion of objects within walls were obtained by Demiański et al. (2000) many details were discussed later on.

The mean characteristics of observed LSS were found in Doroshkevich et al. (2004) for the DR1 SDSS (186 240 galaxies). The typical size of low density regions was found as $\langle D_f\rangle \approx 10-30h^{-1}Mpc$ for filaments with various richness. For walls the mean separation $\langle D_w\rangle \sim 60h^{-1}Mpc$, the surface density and internal velocity dispersion were found.

The spatial distribution of intergalactic baryons is found to be more homogeneous than the luminous matter. Thus, the mean comoving separation of Ly-$\alpha$ forest was found at $z\geq 2$ as $\langle D_\alpha\rangle \sim 21(1+z)^{-2}h^{-1}Mpc$. The observations of the Ly-$\alpha$ forest within voids at small redshifts (Penton et al 2000, 2002) confirm this inference.

## Selection criterion

The most unbiassed characteristic of Low Density Regions (LDRs, voids) is the distance between structure elements of a selected sample along a set of random straight lines. Many popular descriptions of voids such as the Void Probability Function or Voidfinder use additional artificial restrictions of the shape of selected regions. Voids (LDRs) are occupied by single and bynary galaxies and by poor LSS elements. Thus, the Boötes void contains $\sim 26$ late–type, gas–rich galaxies combined to loose pairs and groups (Cruzen et al 2002).

We use MST to select subsamples of LDRs. **If we throw away "clusters" with tree edge lengths $l<l_{thr}$ and richness $N>1$ we achieve a sample of isolated objects.** The question is what is the "good" value of $l_{thr}$. We use halo catalog from a moderate resolution N-BODY DM simulation to address this question.

For each halo we compute the mean expansion velocity of matter in a sphere of radius 5 $h^{-1}$ Mpc. We also use MST to select particles which belong to the joint LSS network, which contains about 50% of matter. Throwing away these particles leaves the LDRs (void).

From the Figs. 1 & 2 it is clear that $l_{thr}=4-5h^{-1}$ Mpc yields halos in expanding regions. However, for any threshold link large fraction of isolated halos belongs to the interconnected LSS network. It is important that the behavior of these two graphs in the range $l_{thr}=3-5h^{-1}$ Mpc is the same for different halo masses that we used. With such value of $l_{thr}$ our criterion is also not affected by the Finger of God effect.

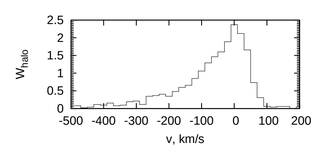


Figure 1. The PDF of a halo to be in expanding ($v>0$) or contracting ($v<0$) environment. Total amount in expanding environment is 25%.

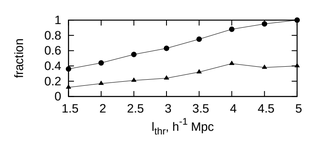


Figure 2. The fraction of isolated halos which are simultaneously: 1) in expanding regions (circles); 2) LDRs (triangles).

| Sample | N | $n$, h Mpc$^{-1}$ | $N_{isol}$ | $f_{isol}$ |
|---|---|---|---|---|
| SDSS, $10<D<100$ | 79145 | 0.10 | 173 | $2.2\cdot10^{-3}$ |
| $M>10^{10}$ | 33819 | 0.27 | 0 | 0 |
| $M>3.5\cdot10^{10}$ | 11826 | 0.10 | 0 | 0 |
| $M>2\cdot10^{11}$ | 2511 | 0.02 | 7 | $3\cdot10^{-3}$ |

### Mass threshold

The table to the left shows that by choosing a halo mass threshold it is impossible to fit the number density of galaxies and the fraction of isolated objects simultaneously. This demonstrates the overabundance problem of $\Lambda$CDM. We choose to fit the fraction.

Table 1. Full samples of galaxies and subsamples with $M_r>-16$

| | $D_{min}$ | $D_{max}$ | $N_{gal}$ | $\langle n_{gal}\rangle$ | $\langle M_u\rangle$ | $\langle M_g\rangle$ | $\langle M_r\rangle$ | $\langle M_i\rangle$ | $\langle M_z\rangle$ |
|---|---|---|---|---|---|---|---|---|---|
| full samples | | | | | | | | | |
| $S_1$ | 10 | 100 | 79 145 | 0.11 | -13.7 | -15.1 | -15.8 | -16.1 | -16.3 |
| $S_2$ | 100 | 200 | 225 063 | 0.044 | -15.1 | 16.7 | -17.5 | -18.0 | -18.2 |
| $S_3$ | 200 | 300 | 215 921 | 0.015 | -15.7 | -17.4 | -18.4 | -18.8 | -19.2 |
| Subsamples with $M_r>-16$ | | | | | | | | | |
| $S_{11}$ | 10 | 100 | 43 664 | 0.061 | -13.0 | -14.2 | -14.8 | -15.0 | -15.2 |
| $S_{21}$ | 100 | 200 | 6 774 | 0.003 | -13.9 | 15.2 | -15.7 | -16.0 | -16.2 |

Table 2. Samples of galaxies within low density regions

| | $N_{gal}$ | $\langle M_u\rangle$ | $\langle M_g\rangle$ | $\langle M_r\rangle$ | $\langle M_i\rangle$ | $\langle M_z\rangle$ |
|---|---|---|---|---|---|---|
| $L_{13}$ | 424 | -14.0 | -15.3 | -15.9 | -16.2 | -16.4 |
| $L_{11}$ | 173 | -13.9 | -15.1 | -15.7 | -15.9 | -16.2 |
| $L_{23}$ | 412 | -15.4 | -16.9 | -17.6 | -18.0 | -18.3 |
| $L_{21}$ | 223 | -15.3 | -16.8 | -17.5 | -17.9 | -18.2 |
| $L_{33}$ | 3 460 | -15.9 | -17.5 | -18.4 | -18.9 | -19.2 |
| $L_{31}$ | 1 698 | -15.9 | -17.5 | -18.4 | -18.8 | -19.2 |

Here samples $L_{13},\ L_{23}\,\&\,L_{33}$ contain single, binary galaxies and triplets, while samples $L_{11},\ L_{21}\,\&\,L_{31}$ contain the single galaxies only.

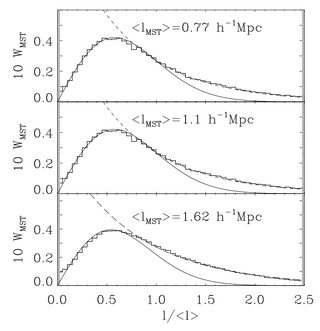


Figure 3: The PDFs for MST edge lengths for three subsamples $S_1$, $S_2$, & $S_3$ of the SDSS DR7 (top, middle and bottom). Fits are plotted by the solid and dashed lines. The functions $W_{MST}$ are well fitted by the superposition of Rayleigh ($\sim 60\%$ of galaxies) and exponential($\sim 40\%$ of galaxies) functions

$$W_R=1.2x\exp(-1.5x^2),\quad W_E=1.2\exp(-1.5x)\,,$$

for samples $S_1$ & $S_2$, and for $S_3$

$$W_R=1.2x\exp(-1.7x^2),\quad W_E=\exp(-1.3x)\,.$$

These results confirms the high degree of concentration of galaxies within the walls and filaments formed the network of the LSS.

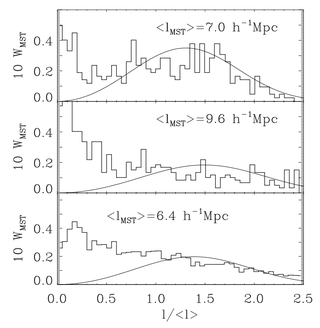


Figure 6. The PDFs for MST edge lengths for low density samples $L_1$, $L_2$, & $L_3$ (top, middle and bottom panels). Fits $W_{MST}\propto x^2\exp(-ax^3)$ are plotted by thin solid lines.

Table 3. Samples of halos with $M>2\cdot10^{11}M_\odot$.

| | *selection* | $N(z=0)$ |
|---|---|---|
| $H_1$ | none | 2511 |
| $Hi_1$ | $l>5,\ N<2$ | 7 |
| $Hi_2$ | $l>4,\ N<2$ | 25 |
| $HL_1$ | $l>4,\ N<4$ | 43 |

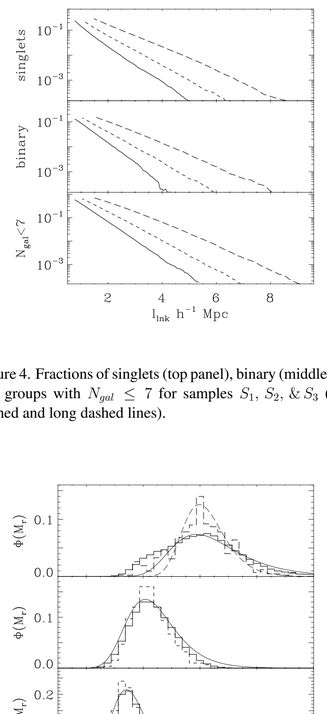


Figure 4. Fractions of singlets (top panel), binary (middle panel) and groups with $N_{gal}\leq 7$ for samples $S_1$, $S_2$, & $S_3$ (solid, dashed and long dashed lines).

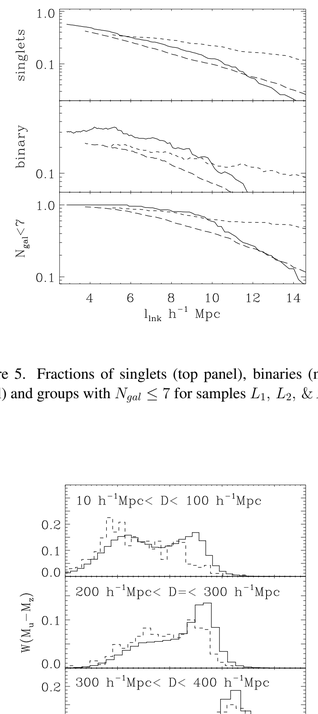


Figure 5. Fractions of singlets (top panel), binaries (middle panel) and groups with $N_{gal}\leq 7$ for samples $L_1$, $L_2$, & $L_3$ .




Figure 7. The luminosity functions for $M_r$ for samples $S_1$, $S_2$, & $S_3$ (solid lines) and $L_1$, $L_2$, & $L_3$ (dashed lines) are plotted together with fits




Figure 8. The PDFs for $M_u-M_z$ for samples $S_1$, $S_2$, & $S_3$ (solid lines) and $L_1$, $L_2$, & $L_3$ (dashed lines).

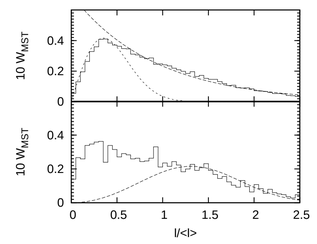


Figure 9. The PDFs for MST edge lengths for the full sample of halos $H_1$ (top) with fits $W_R=0.97x\exp(-2x^2)$, $W_E=0.7\exp(-1.1x)$, and for the low density sample (bottom) $HL_1$ with fit $W\propto x^2\exp(-0.3x^3)$.

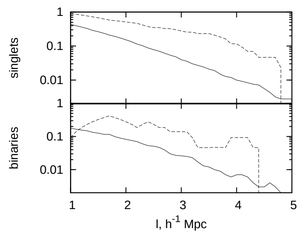


Figure 10. Fractions of singlets and pairs in the full halo catalog $H_1$ (solid) and low density sample $HL_1$ (dashed).

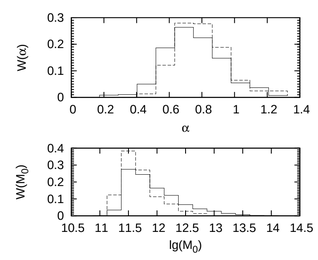


Figure 11. The PDFs for the mass growth fitting parameters, $M_0$ and $\alpha$ ($M(z)=M_0\exp(-\alpha z)$). Solid is for $H_1$ sample and dashed for $HL_1$.

ASC LPI

# Observed voids in the SDSS DR7

The PDFs of MST edge lengths for subsamples $S_1$, $S_2\,\&\,S_3$ are given in Table 1 are plotted in Fig. 3. For all samples these PDFs demonstrate similar galaxy distribution $W_{MST}(x)$, $x=\ell_{MST}/\langle\ell_{MST}\rangle$ with a slow increase of $\langle\ell_{MST}\rangle$ with distance.

For comparison the PDFs of the MST edge lengths found for the LDRs with the size $D_v\geq 2l_{thr}=10h^{-1}Mpc$ selected in the samples $S_1$, $S_2$, & $S_3$ are presented in Fig. 6 (top, middle and bottom panels) together with function

$$W_{MST}\propto x^2\exp(-bx^3),\quad x=\ell/\langle\ell\rangle\,, \tag{1}$$

described the PDF for the randomly distribute objects. Strong excess of objects with small separation indicates contribution of pair, triplets and poor groups of galaxies. Main characteristics of these subsamples, $L_1$, $L_2$, & $L_3$, are listed in Table 2.

For the full samples $S_1$, $S_2$, & $S_3$ the fractions of single and binary galaxies and groups with $N_{gal}\leq 7$ are plotted in Fig. 4 vs. the distance to the nearest neighbor (the linking length $\ell_{lnk}$). All these functions are well fitted by exponential functions

$$f\propto\exp(-\ell_{lnk}/\ell)\,, \tag{2}$$

with $\ell=0.6\,0.7,\ \&\,0.9h^{-1}Mpc$

For comparison, for the LDR samples $L_1$, $L_2$, & $L_3$ the fractions of single and binary galaxies and the poor groups of galaxies with $N_{gal}\leq 7$ are plotted in Fig 5. The domination of pair of galaxies is clearly seen as an excess of closer objects.

For DM particles situated within low density regions of simulation at $z=0,1,2,\,\&\,3$ the PDFs of the MST edge length plotted in Fig. are well fitted by (1) with $b(z)=0.78;1.5;2.53;\&3$..

## Spectral characteristics

The luminosity functions, $\Phi_r$, for samples $S_1$, $S_2$, & $S_3$ and $L_1$, $L_2$, & $L_3$ are plotted in Fig. 7 together with the standard fit

$$\Phi_{M_r}=0.921\Phi^*\eta^{\alpha+1}\exp(-\eta),\quad \eta=10^{0.4(M^*-M_r)}\,, \tag{3}$$

Fit parameters for the samples $S_1$, $L_1$, $S_2$, & $S_3$ are $\Phi^*=0.217,0.195;0.326;0.11$, $\alpha=-0.07,1.33;0.7;2.4$, $M^*=-16.2,-15.1;-17.35;-17.26$. Significant differences are seen only between samples $S_1\,\&\,L_1$ which contain larger fraction of galaxies with $M_r\geq -16$. For the same samples $S_1$, $S_2$, & $S_3$ and $L_1$, $L_2$, & $L_3$ the PDFs for the $M_u-M_z$ are plotted in Fig. 8. Comparison of these PDFs confirms some excess of late–type galaxies for the closest regions, $S_1\,\&\,L_1$. For distant regions this excess progressively decreases.

# Properties of isolated halos

For our analysis we use the 50 $(h^{-1}$ Mpc$)^3$, $512^3$ DM particles simulation from the MareNostrum Universe project. The main properties of halo samples are presented in Table 3, and the PDFs for MST edge lengths are plotted in Fig. 9.

## Halos and LSS

The LSS was selected from simulation particles by MST as one interconnected cluster with overdensity $\delta_{thr}=1.2$, it comprises 50% of particles. 92% of halos in $H_1$ sample belongs to this LSS. As high as 60% of isolated halos from $Hi_{1,2}$ are also incorporated in the LSS. This demonstrates the common property of $\Lambda$CDM: **voids are filled with weak filaments on which halos reside**.

## Dynamical properties of environment

We compute the expansion rate of environment as a mean projection of matter velocity to the radius of a $5h^{-1}$ Mpc sphere around each halo. The distribution of this characteristic for all halos is presented in Fig. 1. We also compute dipole and quadrupole spherical harmonics of projected velocity. This gives a quantitative description of anisotropy of environment expansion. We find that **dipole and quadrupole amplitudes are about 16% and 17% of monopole**.

## Halo evolution

The mass growth of a halo is known to be well fitted by function $M(z)=M_0\exp(-\alpha z)$. We derive parameters $M_0$ and $\alpha$ for samples $H_1$ and $Hi_{1,2}$ and find that $\alpha$ is almost equal for both samples, while isolated halos demonstrate 1.5 times lower mean $M_0$. The PDFs for $M_0$ and $\alpha$ are shown in Fig 11.

The merger rate for isolated halos is approximately 1.5 times lower than for $H_1$ halos.

# Conclusions

Properties of isolated galaxies are strongly dependent upon the criteria used for the sample selection. The Minimal Spanning Tree tehnique allows to select samples of isolated objects and groups of objects from observed and simulated catalogs. A good choice of the only selection parameter — the distance to the nearest neighbour — is $4-5h^{-1}$ Mpc. Samples of isolated simulated halos demonstrate lower mass, rare mergers and expanding environment. In SDSS DR7 the sample of nearby isolated galaxies with distances $10<D<100h^{-1}$ Mpc shows the most prominent differences from the full sample: isolated galaxies are somewhat bluer and fainter than normal. It would be interesting to observe the HI and metal absorption lines near the isolated galaxies.